
Article:
Marulanda-Durango, J., Escobar-Mejía, A., Alzate-Gómez, A. et al. (1 more author) (2021) A support vector machine based method for parameter estimation of an electric arc furnace model. Electric Power Systems Research, 196. 107228. ISSN 0378-7796

https://doi.org/10.1016/j.epsr.2021.107228

A Support Vector Machine-Based Method for Parameter Estimation of an Electric Arc Furnace Model

J. Marulanda-Durango[a,*], A. Escobar-Mejía[a], A. Alzate-Gómez[a], M. Álvarez-López[b]

[a] *Electrical Engineering Program, Universidad Tecnológica de Pereira, Pereira, Colombia*
[b] *Department of Computer Science, University of Sheffield, Sheffield, UK*

Abstract

In the iron and steel industry, electric arc furnaces (EAFs) are used in the melting and refining process of metals. They are known to demand large amounts of reactive power and cause significant power quality (PQ) problems due to their highly non-linear time varying voltage-current characteristic. Several EAF models have been proposed with the purpose to predict the voltage and current waveforms, to assess the performance of different compensating devices such as static var compensator, synchronous static compensator, active power filters, and –still under study– energy storage systems, and also for planning the installation of iron and steel facilities considering existing real data from similar facilities. An important aspect of these models is related to the estimation of their parameters. This paper presents a new method to estimate the parameters of an EAF model. The method utilizes a multiple-input multiple-output regressor based on support vector machine, that maps from voltage characteristics of the electric arc to the values of the model parameters. The multidimensional support vector regressor (M-SVR) is designed in the training phase, using data from several simulations of the EAF model. These simulations are carried out adjusting the parameters of the model within the search space, and considering the real arc current as input to the model. Then, in the validation phase, for the real voltage waveform, the estimated parameters are obtained using each regressor of the M-SVR. The proposed method is validated by the comparison between the waveforms obtained using the EAF model with actual data from a steel plant. Results show that the relative error between the fundamental component of the current and voltage, for real and simulated waveforms, are 2.1% and 6.3% respectively.

Keywords: Parameter estimation, ac electric arc furnaces, power quality problems, support vector machine, multivariate regression.

*Corresponding author
Email addresses: jjmarulanda@utp.edu.co (J. Marulanda-Durango), andreses1@utp.edu.co (A. Escobar-Mejía), alalzate@utp.edu.co (A. Alzate-Gómez), mauricio.alvarez@sheffield.ac.uk (M. Álvarez-López)

1. Introduction

Electric arc furnaces (EAFs) have been widely used in the steelmaking industry to melt metallic scraps and refining metals. The electrical energy demand can be up to 150 MW [1], and is converted to heat by the electric arc established between electrodes and the melting scrap. The high temperature (reaching several thousand degrees celsius), generates enough heat to melt the scrap [2].

It is well known that the operation of an arc furnace causes power quality (PQ) problems (e.g., harmonics, interharmonics, voltage fluctuations, flickers, etc) in the supply network [3], [4]. This is mainly produced by both its intrinsic nonlinearity and the randomness associated with boring and melting periods [5], [6]. In order to predict and minimize the PQ disturbances, it is necessary for electric utilities and customers to implement strategies to solve PQ problem. Innovative approaches are related to absorption prediction and these techniques require an accurate EAF model. However, modeling is not a straightforward task and requires complex algorithms for parameter estimation [7].

Different techniques have been reported in the literature for modeling the electric arc. In [1], a variable resistor and an inductor connected in series, and a current source to inject harmonics are used to model the electric arc at the primary side of the EAF's transformer. The model is based on field measurements of voltage and current. In [2], the electric arc is modeled as a resistor in series with an inductor, and a parallel-connected capacitor to reduce the error of the model compared to the measured parameters. The arc resistance is modeled as a nonlinear time-variant resistance considering stochastic variation of both the arc length [8] and the arc voltage [9]. In [10] and [11], a time domain model, based on a non-linear differential equation derived from the energy conservation principle, is proposed. Two previous electric arc models have merged into a single model in [12] to generate a new time domain exponential and hyperbolic model. Several models use a low frequency chaotic signal to take into consideration the chaotic dynamics of an electric arc [13–16]. Other models also include deterministic signals, like a sine function [12], [17], or a stochastic signal, like as band-limited white noise [12], [17], [18], to account for fluctuations in the electric arc length. A nonlinear conductance function based on cubic spline interpolation and field measurements of voltages and currents is used in [19] to model an electric arc in the steady-state. A frequency-domain model is proposed in [20] for iterative harmonic analysis. In [21], an electric arc model has been presented, based on hidden Markov theory, to generate different operating points of the voltage-current ($v-i$) characteristic in the form of probability distribution. Other approaches for modeling the dynamic $v-i$ relationship of the electric arc, include the use of radial basis function neural networks [22–26], and neuro-fuzzy rule-based networks [3].

It is worth noting that an important aspect of the electric arc models is related to the estimation of their parameters. In [8], the parameters of the model are determined using a trial and error procedure by matching the simulated active power and short-term flicker severity (Pst) with real measurements. An empirical relationship that relates transformer taps and the distance between electrodes is used in [2], to

determine the values of the arc impedance. In [1], the resistor and inductor values are constantly updated, by computing the magnitude and the angle of the current and voltage at the fundamental frequency. In [15] the tuning process of the model parameters consists of finding values in a search space that minimize an objective function. In [7] and [9], a two-step optimization technique based on a genetic algorithm has been proposed to estimate the parameters of the nonlinear time-varying electric arc model, incorporating the stochastic variation of the arc length. A differential evolution algorithm is used in [11] to estimate the values of the parameters of the nonlinear differential equation that relates the arc conductance, arc current and arc length. A parameter estimation of the Generalized Cassie-Mayr EAF model [27] is presented in [28], using the least-mean square method with real current and voltage measurements. In [29], the interior-point method is used to identify the electric arc parameters of the power balance equation for the mathematical model derived in [10], this is achieved finding a closed form analytical solution of the equation. In [30] a set of parameters of the model are chosen by determining the power factor for a particular case study.

This paper proposes a novel method based on support vector machines (SVMs) to estimate the parameters of an electric arc model. The SVM is used for building a multiple-input multiple-output regressors called support vector regression (M-SVR). The main motivations to use the M-SVR method are advantages such as: the ability to estimate the parameters with limited data, robust predictions when nonlinearities and noise appear in the system [31], and considering all the inputs and outputs together to construct each regressor. The electric arc model, based on chaotic dynamics, is implemented in Matlab/Simulink and is used to get several voltage waveforms, using different values for the model parameters in each simulation. The values of each set of parameters are obtained using latyn hypercube sampling (LHS) [32]. Data from simulation are then used to design the M-SVR, that maps from the voltage characteristics of the electric arc to the values of the electric arc model parameters. The characteristics are computed using the short-time Fourier transform (STFT), considering the harmonics and interharmonics of the obtained voltage waveforms. The hyperparameters of the M-SVR have been adjusted using the differential evolution (DE) algorithm [33]. Once the M-SVR has been designed, the parameter estimation for a real voltage waveform is achieved by mapping its characteristic to the values of the parameters. This is achieved using each regressor of the multidimensional regressor. The proposed method here have some advantages over the proposals in [7] and [9] such as: compact solution by considering all the parameters at the same time, and fast response once the M-SVR has been designed.

This paper is organized as follows. Section 2 presents the description of the EAF power system and the real measurements used for the parameters estimation. Section 3 presents a description of the non-linear time-varying electric arc model, while the proposed method to estimate the model parameters is described in Section 4. Also, this section provides a description of the M-SVR. The validation of the proposed method is presented in Section 5, and finally conclusions and remarks are given in Section 6.

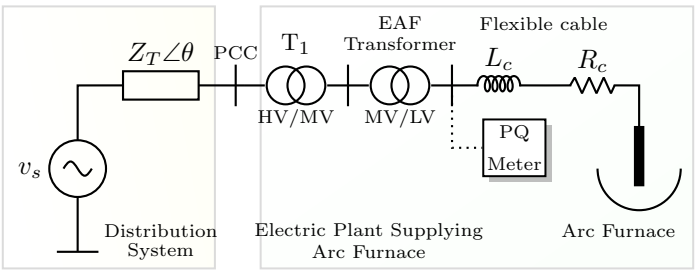

Figure 1: Single-phase diagram of the EAF power system under study.

2. EAF power system and real data

Fig. 1 shows the single-phase diagram of the power system used for to connect a 40 tonnes EAF with the power grid. The distribution network is modeled using an equivalent Thevenin circuit. The Thevenin equivalent comprises a three-phase stiff voltage source in series with a Thevenin impedance $Z_T\angle\theta$, computed from the short-circuit power at the point of common coupling (PCC). The EAF is connected to the distribution network through two power transformer: a high voltage/medium voltage (HV/MV) T_1 transformer, and medium voltage/low voltage (MV/LV) called EAF transformer, which has a tap changer in the secondary winding to set the power delivered to the furnace. The electrodes are connected to the secondary side of EAF transformer through of flexible cables and bus tubes, which constitutes nearly of 75% of the total impedance of EAF facility. The parameters of the EAF power system shown in Fig. 1 are listed in Appendix A.

In this study, real measurements of line current and phase voltage taken at the secondary side of the EAF transformer during the melting stage of the EAF operation, are used for the parameters estimation of the electric arc model. A PQ meter (AEMC 8333 Power Pad III) connected at phase A of the secondary windings of EAF transformer, was used to measure 100 cycles at 50 Hz, and at a sampling rate of 256 samples per cycle.

Considering [1], the magnitude and the angle of the sinusoidal internal phase voltage v_s are found by using the current and phase voltage measurements referred at the HV side of the transformer T_1, and considering the leakage reactance and the turn ratio of both transformers. The sinusoidal internal voltage v_s is computed by extracting the fundamental component of the resulting voltage obtained by summing the phase voltage at the PCC and the voltage drop on the Thevenin impedance, which is caused by line current. This calculation is done before estimating the electric arc model parameters.

The current and voltage measurements are necessary to be normalized for the convergence algorithms of the M-SVR, using 1000 A and 1000 V as a base.

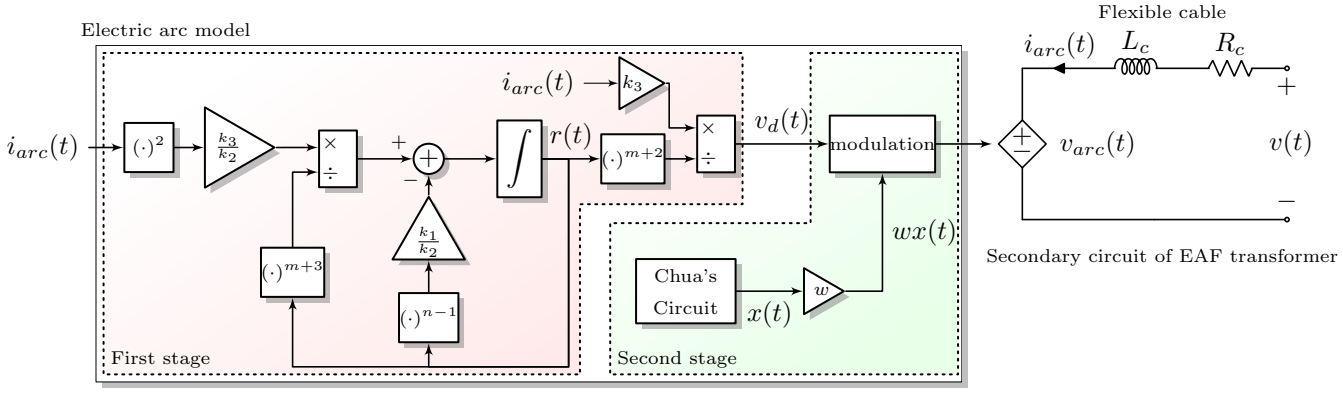

Figure 2: Block diagram of the dynamic behavior of electric arc including chaotic signal.

3. Electric arc model

In this paper the dynamic model of the electric arc presented in [14] is used. The electric arc is modeled as a current controlled voltage source that comprises two stages as illustrated in Fig. 2: a non-linear dynamic $v-i$ characteristic of the electric arc (first stage) and a chaotic voltage fluctuation (second stage) to represent the flicker effect in the voltage waveforms at the PCC.

Initially, the radius of the electric arc $r(t)$ is calculated using the non-linear differential equation derived from the energy conservation principle as follows:

$$k_1 r^n + k_2 r \frac{dr}{dt} = \frac{k_3}{r^{m+2}} i_{arc}^2, \tag{1}$$

where i_{arc} is the arc current, k_1 is proportional to the power transmitted as heat to the external environment, the parameter k_2 is proportional to the internal energy of the electric arc, and the parameter k_3 is inversely proportional to the resistivity of the arc column [10]. Notice that, k_1, k_2 and k_3 depends on the energy of the electric arc, being equal to the product of the arc voltage and the arc current. The parameters m and n enable different $v-i$ characteristics. The possible combinations of these parameters for the different stages of the arcing process are found in [10]. The deterministic electric arc voltage $v_d(t)$ is obtained from $r(t)$ using

$$v_d = \frac{k_3}{r^{m+2}} i_{arc}. \tag{2}$$

At the second stage, the instantaneous values computed for $v_d(t)$ are modulated in amplitude through a low frequency chaotic signal. The modulated signal is the electric arc voltage and is referred as $v_{arc}(t)$,

$$v_{arc} = v_d(1 + wx), \tag{3}$$

where w is the gain factor of a low frequency chaotic signal $x(t)$, generated by Chua's circuit, whose equations are given by [34]:

$$\begin{aligned}
\frac{dx}{dt} &= \begin{cases} s\alpha(y - \kappa x + \rho - \kappa), & \text{if } x < -1 \\ s\alpha(y - \rho x), & \text{if } -1 \leq x \leq -1 \\ s\alpha(y - \kappa x - \rho + \kappa), & \text{if } x > 1 \end{cases} \\
\frac{dy}{dt} &= s(x - y + z) \\
\frac{dz}{dt} &= -s\delta y
\end{aligned} \tag{4}$$

where $x(t)$, $y(t)$ and $z(t)$ are the state variables, s is a time scale factor used for adjusting the frequency of $x(t)$, and w is the gain factor of $x(t)$ that is related with the severity of the voltage fluctuations caused by arc length variation [7]. Following the idea presented in [15], the values of ρ, κ, α and δ, are adjusted in a range of values that produce the chaotic behavior of Chua's circuit [15].

The voltage signal $v_{arc}(t)$ is connected to the electrical power system as a current controlled voltage source. In practice, the voltage measurements are taken at the secondary side of the EAF transformer. The simulated voltage at this place is referred as $v(t)$, and according to the circuit shown in Fig. 2, its value is calculated as

$$v = R_c i_{arc} + L_c \frac{di_{arc}}{dt} + v_{arc}, \tag{5}$$

where R_c and L_c are the resistance and inductance respectively, of the secondary circuit including flexible cables, bus tubes and the impedance of the electrode, and in this study they are part of the parameters to be estimated. The electric arc model is implemented in Matlab/Simulink. In brief, the arc furnace model behaves a current controlled voltage source, which takes as input the arc current. With this current and the estimated parameters, the arc voltage $v(t)$ is calculated every time-step.

4. Parameter estimation of the electric arc model

This section presents the proposed method used to estimate the parameters of the electric arc model described in Section 3. First, a short description of the M-SVR is given in subsection 4.1. Then, subsection 4.2 explains the differential evolution algorithm used to determine the hyperparameters of the M-SVR. Finally, a detailed description of the proposed method to estimate the parameters of the electric arc model is presented in subsection 4.3.

4.1. Multidimensional regression based on SVM

This subsection provides a description of the SVM regression-based method for multiple-input multiple-output. This method was initially proposed in [31], and is called support vector multiregressor or M-SVR. The objective of the multidimensional regression problem is to find the mapping between an input vector $\mathbf{x} \in \mathbb{R}^d$ and an observable output vector $\mathbf{y} \in \mathbb{R}^Q$, from a given set of independent and identically distributed (i.i.d.) samples $\{(\mathbf{x}_i, \mathbf{y}_i)\}_{i=1}^N$. The relationship between $\mathbf{x}$ and $\mathbf{y}$ is assumed as follows

$$\mathbf{y} = \mathbf{W}^\top \boldsymbol{\phi}(\mathbf{x}) + \mathbf{b}, \tag{6}$$

where $\mathbf{W} = \left[\mathbf{w}^1, \ldots, \mathbf{w}^Q\right]$, $\mathbf{b} = \left[b^1, \ldots, b^Q\right]^\top$, with a vector $\mathbf{w}^j \in \mathbb{R}^{\mathcal{H}}$ and a constant b^j, for every output ($j = 1, \ldots, Q$). The function $\boldsymbol{\phi}(\cdot)$ refers to a non-linear transformation to a higher-dimensional Hilbert space $\mathcal{H}$, where $\mathcal{H} \gg d$.

In the M-SVR, the parameters $\mathbf{w}^j$ and b^j are found by minimizing the convex functional,

$$J = \frac{1}{2} \sum_{j=1}^{Q} \|\mathbf{w}^j\|^2 + C \sum_{i=1}^{N} L(u_i), \tag{7}$$

where the hyperparameter C is a regularization constant, $L(\cdot)$ is the Vapnik $\epsilon-$ insensitive loss-function, with $u_i = \|\mathbf{e}_i\|$, and $\mathbf{e}_i = \mathbf{y}_i - \mathbf{W}^\top \boldsymbol{\phi}(\mathbf{x}_i) - \mathbf{b}$. As a loss function $L(\cdot)$, authors in [31] use a quadratic function with respect to a hyperparameter ϵ, as follows

$$L(u_i) = \begin{cases} 0, & u_i < \epsilon \\ (u_i - \epsilon)^2, & u_i \geq \epsilon. \end{cases} \tag{8}$$

where $\epsilon \neq 0$. By using the Representer Theorem [35], the solution of the problem above is expressed in terms of the vector of coefficients $\boldsymbol{\beta}^j \in \mathbb{R}^n$ for each output [31], which relates to the original vectors $\mathbf{w}^j$ through $\mathbf{w}^j = \boldsymbol{\Phi}^\top \boldsymbol{\beta}^j$, where $\boldsymbol{\Phi} = [\boldsymbol{\phi}(\mathbf{x}_1), \ldots, \boldsymbol{\phi}(\mathbf{x}_N)]^\top$.

An iterative reweighted least squares procedure is proposed in [31] to minimize J, in order to calculate the set of regressors $\boldsymbol{\beta} = \left[\boldsymbol{\beta}^1, \ldots, \boldsymbol{\beta}^Q\right]$ and $\mathbf{b}$. To compute the regressors at the $(p+1)^{\text{th}}$ iteration, initially is necessary to calculated the descending direction of J, based on the optimal solution of its quadratic approximation, refer as $\boldsymbol{\beta}^s$ and $\mathbf{b}^s$ and given by [31]

$$\begin{bmatrix} \boldsymbol{\beta}^s \\ (\mathbf{b}^s)^\top \end{bmatrix} = \begin{bmatrix} \mathbf{K} + \mathbf{D}_a^{-1} & \mathbf{1} \\ \mathbf{a}^\top \mathbf{K} & \mathbf{1}^\top \mathbf{a} \end{bmatrix}^{-1} \begin{bmatrix} \mathbf{Y} \\ \mathbf{a}^\top \mathbf{Y}, \end{bmatrix} \tag{9}$$

where $\mathbf{K} \in \mathbb{R}^{N\times N}$ is a kernel matrix with entries $k(\mathbf{x},\mathbf{x}') = \boldsymbol{\phi}(\mathbf{x})^\top \boldsymbol{\phi}(\mathbf{x}')$ computed from a so called kernel function k, and $\mathbf{Y} = [\mathbf{y}_1,\ldots,\mathbf{y}_N]^\top$. The kernel function generalizes the inner product between $\boldsymbol{\phi}(\mathbf{x})$, and $\boldsymbol{\phi}(\mathbf{x}')$. [1] Also, in (9), $\mathbf{a} = [a_1,\cdots,a_N]^\top$, and $\mathbf{D}_a \in \mathbb{R}^{N\times N}$ is a diagonal matrix with entries $\{a_i\}_{i=1}^N$. The weights a_i are computed using

$$a_i = \frac{C}{u_i^p}\frac{dL}{du}\bigg|_{u_i^p} = \begin{cases} 0, & u_i^p < \epsilon \\ \frac{2C(u_i^p-\epsilon)}{u_i^p}, & u_i^p \geq \epsilon \end{cases} \tag{10}$$

where $u_i^p = \|\mathbf{e}_i^p\|$. The next step solution $\boldsymbol{\beta}^{p+1}$ and $\mathbf{b}^{p+1}$, can be estimated by:

$$\begin{bmatrix} \boldsymbol{\beta}^{p+1} \\ (\mathbf{b}^{p+1})^\top \end{bmatrix} = \begin{bmatrix} \boldsymbol{\beta}^{p} \\ (\mathbf{b}^{p})^\top \end{bmatrix} + \eta^p \begin{bmatrix} \boldsymbol{\beta}^{s} - \boldsymbol{\beta}^{p} \\ (\mathbf{b}^{s} - \mathbf{b}^{p})^\top \end{bmatrix}, \tag{11}$$

where the value of η^p is computed using a backtracking algorithm, in which, if $J^{p+1} > J^p$, then η^p is multiplied by a positive constant less that one, and the regressors $\boldsymbol{\beta}^{p+1}$ and $\mathbf{b}^{p+1}$ are computed again, until a decrease is achieved in J^{p+1}. The algorithm stops when $J^{p+1} - J^p <$ tolerance. In this paper, the tolerance is set to 10^{-9}.

Finally, once the optimal regressors have been calculated, the prediction $\hat{\mathbf{y}}$ for a new input vector $\mathbf{x}$ can be computed as

$$\hat{\mathbf{y}} = \boldsymbol{\beta}^\top \mathbf{k}_{\mathbf{x}} + \mathbf{b}, \tag{12}$$

where $\mathbf{k}_{\mathbf{x}} \in \mathbb{R}^N$ is a vector with entries given by $\mathbf{k} = \{k(\mathbf{x}_i,\mathbf{x})\}_{i=1}^N$. The kernel function that is used in this paper is the radial basis function (RBF) kernel given as

$$k(\mathbf{x},\mathbf{x}') = \exp\left(-\frac{\|\mathbf{x}-\mathbf{x}'\|^2}{2\sigma^2}\right), \tag{13}$$

where the hyperparameter σ^2 is usually known as the bandwidth [36].

4.2. Differential evolution algorithm

As described in subsection 4.1, the M-SVR has the hyperparameters C, ϵ, σ, which should be optimized in order to let the M-SVR estimate the parameter of the electric arc model. In this paper, the differential evolution (DE) algorithm is used to determine the values of these hyperparameters.

[1] In the sense that the kernel is not necessarily a Mercer kernel, this is, one that can be written as an inner product. See Ref. [36].

The DE algorithm was proposed in 1997 by Storn and Price [33] as a metaheuristics optimization algorithm, which maintains a population of potential solutions in the search space by applying the idea of survival of the fittest. In this case, the search space is formed by predefined intervals for values of M-SVR hyperparameters. The main advantages of DE is its convenient implementation, lack of a differentiable cost function, good converge properties, and few control variables to achieve the minimization.

The DE algorithm makes use of three main rules: mutation, crossover, and selection. Initially, a population of size N_p is generated. Each individual of the population has the following structure:

$$\mathbf{h}^g = [C^g, \epsilon^g, \sigma^g] \tag{14}$$

where g represent the g^{th} generation.

The mutation rule creates a mutant vector in each generation following the rule:

$$\hat{\mathbf{h}}^{g+1} = \mathbf{h}_1^g + F(\mathbf{h}_2^g - \mathbf{h}_3^g) \tag{15}$$

where F is a mutation factor in the range $[0, 1.2]$, and $\mathbf{h}_1^g$, $\mathbf{h}_2^g$, $\mathbf{h}_3^g$, are three random vectors taken from the population in the g^{th} generation.

The crossover rule generates a trial vector $\mathbf{h}^{g+1}$, where each one of its entries are computed as follows:

$$h_j^{g+1} = \begin{cases} \hat{h}_j^{g+1}, & \text{if } \vartheta \leq CR \\ h_j^g, & \text{otherwise} \end{cases} \tag{16}$$

for $j = 1, 2, 3$. ϑ is a random variable which follows a normal distribution in the range $[0, 1]$, and CR is know as crossover constant.

The selection rule compares the value of the objective function (OF) for the trial vector and the OF for the target vector $\mathbf{h}^g$, and select the best solution that is stored in the population for the next generation $(g + 1)$, as follow

$$\mathbf{h}^{g+1} = \begin{cases} \mathbf{h}^{g+1}, & \text{if OF}(\mathbf{h}^{g+1}) \leq \text{OF}(\mathbf{h}^g) \\ \mathbf{h}^g, & \text{otherwise} \end{cases} \tag{17}$$

The above procedure is repeated for each individual of the population. The algorithm stops when the number of maximum generations $g^{\max}$ defined by the user is reached. The OF is defined in the following subsection, after introducing the proposed method.

4.3. Proposed method

The proposed method used to estimate the parameters of the electric arc model, requires voltage and current real measurements at the secondary side of the EAF transformer. The 100 cycles of measurements are divided into the first 70 cycles for training, and the last 30 cycles for testing, as shown in Fig. 3.

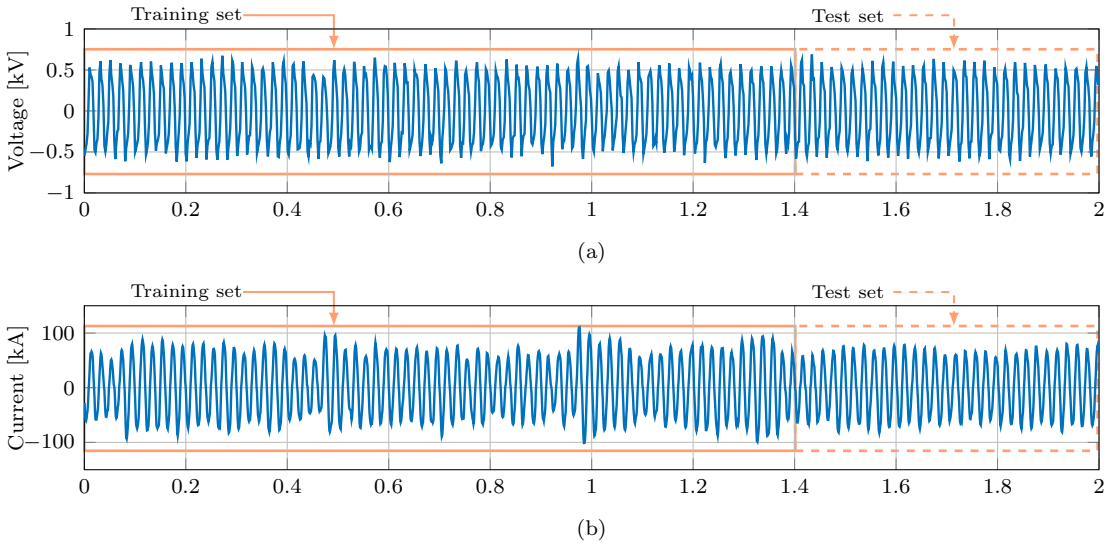

Figure 3: (a) Real measurements of voltage $v(t)$, (continuous lines) training data, (dashed lines) testing data. (b) Real measurements of current $i(t)$, (continuous lines) training data, (dashed lines) testing data.

The method is implemented in the following steps as indicated in the flowchart diagram in Fig. 4. In the first step, the training measurements of the electric arc current are used as input to the electric arc model described in Section 3 (see Fig. 2), in order to get a considerable number of simulated voltage waveforms at the secondary side of EAF transformer $v(t)$, using different values for the model parameters in each simulation. The vector $\mathbf{y} = [y_1, \ldots, y_Q]^\top$ comprises the Q parameters of the electric arc model to be estimated. Using LHS, are generated N different samples for the vector $\mathbf{y}$, where each entry of $\mathbf{y}$ are within the predefined intervals for values of electric arc parameters. In this paper the LHS is used instead of random sampling because the LHS gives good coverage of the space, and are evenly distributed in each one-dimensional projection [32]. Each sample of $\mathbf{y}$ is refer as $\mathbf{y}_i$ $(i = 1, \ldots, N)$. A matrix $\mathbf{Y} \in \mathbb{R}^{N \times Q}$ is used to group the vectors $\{\mathbf{y}_i^\top\}_{i=1}^N$, each row in $\mathbf{Y}$ correspond to a vector $\mathbf{y}_i^\top$.

For the training measurements of the electric arc current and for each vector of parameters $\mathbf{y}_i$ of the electric arc model, a simulation of the electric arc model described in Section 3 is executed. On each waveform of $v(t)$ obtained in each run of the model, a set of characteristics are extract to construct the input vectors $\{\mathbf{x}_i\}_{i=1}^N$ for the M-SVR algorithm. The characteristics used in this paper consist of the harmonics and interharmonics of the voltage waveform, obtained using the STFT [1]. It is worth noting that in this

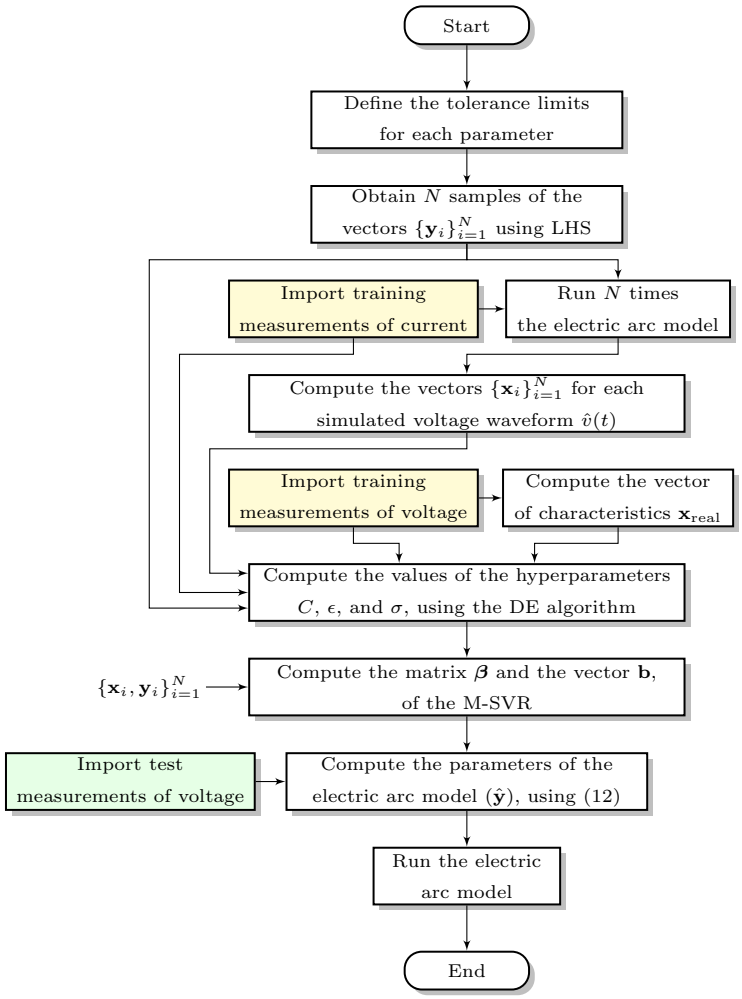

Figure 4: Flowchart diagram of the proposed method.

paper, current and voltage measurements at a fundamental frequency of 50 Hz have been considered. The spectrogram is computed over the voltage waveform using the STFT, where each segment of the signal is windowed with a Hamming window of 5−Hz resolution, with an overlap of 90% between the segments (see Fig. 5).

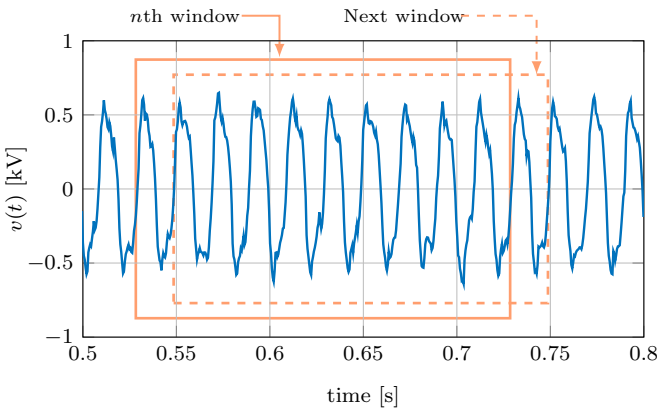

Figure 5: Windowing of the voltage $v(t)$. (Continuos lines) nth window. (Dashed lines) Next window, sliding on the right the nth window by one cycle.

Let N_w be the number of segments or windows in which the voltage signal is segmented. To account for the harmonics and interharmonics of the voltage waveform, the STFT is computed with frequencies between the range of 5 to 650 Hz, with steps of 5 Hz for 5 Hz to 100 Hz, and 50 Hz for larger frequencies [37]. The spectrogram for $v(t)$ is a matrix of dimensions $31 \times N_w$, which is labeled as $\mathbf{S}_i$, where the subscript i is related to the subscript i in the vector $\mathbf{y}_i$. In the rows of $\mathbf{S}_i$, 31 refer to the number of frequency components. For each frequency value, the mean of the magnitude of the spectrogram $\mathbf{S}_i$ is compute across the N_w columns, transforming the matrix $\mathbf{S}_i$ into a vector of dimension 31. This vector is named as $\mathbf{x}_i$. Considering the description given in Section 4.1 for the M-SVR, the value of d is 31. In summary, for each vector of parameters $\{\mathbf{y}_i\}_{i=1}^N$ a vector of characteristics $\{\mathbf{x}_i\}_{i=1}^N$ is computed as explained above.

The second step consists of finding the values of the hyperparameters C, ϵ and σ, for the M-SVR. The hyperparameters are computed using the dataset $\{(\mathbf{x}_i, \mathbf{y}_i)\}_{i=1}^N$, the training measurements of real current and voltage at the secondary side of EAF transformer, and the DE algorithm. As explained in the last subsection, the fitness of the target vector and the trial vector in the DE algorithm, is computed through the OF using (17). In this paper, the OF is calculated as the mean value of the rooted sum of the squared errors, which is the root mean square (RMS) value of the real measured of training voltage at the secondary side of EAF transformer $V_{\text{RMS(real)}}$, and the corresponding RMS value of estimated voltage $V_{\text{RMS(est)}}$ given by the simulation of the EAF model, hence

$$\text{OF} = \frac{1}{N_c}\sqrt{\sum_{i=1}^{N_c}(V_{\text{RMS(est)},i} - V_{\text{RMS(real)},i})^2} \tag{18}$$

where $V_{\text{RMS(real)},i}$ is the RMS value of real measured data, $V_{\text{RMS(est)},i}$ is the RMS value of simulated data, corresponding to the i^{th} cycle, and N_c is the number of cycles of the measured voltage. The simulated

voltage $v(t)$ related to the target vector $\mathbf{h}^g$ is obtained as follows: given fixed values of C^g, ϵ^g and σ^g (the entries of the target vector), and the dataset $\{(\mathbf{x}_i, \mathbf{y}_i)\}_{i=1}^N$ simulated from the electric arc model, are compute $\boldsymbol{\beta}$ and $\mathbf{b}$ using the iterative algorithm explained in subsection 4.1. It is worth noting that, the Matlab source code for computing $\boldsymbol{\beta}$ is available in [38], for further information. Then, the vector of characteristic $\mathbf{x}_{\text{real}}$ is compute from real measurements of training voltage as explained above. By substituting the values of $\boldsymbol{\beta}$, $\mathbf{b}$ and $\mathbf{x}_{\text{real}}$ in (12), the vector $\hat{\mathbf{y}}$ that contains the Q parameters of the electric arc model is estimated. With these parameters and the the training measurements of real current, is run a simulation of the EAF model to obtained the simulated voltage $v(t)$ related to the target vector $\mathbf{h}^g$. The same procedure is repeated to get the simulated voltage related to the entries of the trial vector $\mathbf{h}^{g+1}$. The DE algorithm is stopped when is reached the maximum of generations $g^{\max}$.

The values of the hyperparameters of the M-SVR are adjusted with the corresponding entries of the last target vector. With the optimal values of the hyperparameters of the M-SVR, and the dataset $\{(\mathbf{x}_i, \mathbf{y}_i)\}_{i=1}^N$, are computed the matrix $\boldsymbol{\beta}$ and the vector $\mathbf{b}$, to use in the testing stage.

Finally, given $\boldsymbol{\beta}$, $\mathbf{b}$, and an input vector $\mathbf{x}_{\text{real}}$, it is possible to predict an output vector $\hat{\mathbf{y}}$ using (12). The input vector $\mathbf{x}_{\text{real}}$ represents the characteristics of the real testing voltage waveforms computed using the STFT, and the vector $\hat{\mathbf{y}}$ represents the Q estimated parameters of the EAF model. This estimated values for the electric arc model parameters, are used to get the simulate current and voltage waveform at the secondary side of the EAF transformer.

5. Validation of the proposed approach

This section are divided as following: In subsection 5.1 are designed the M-SVR using the training measurements. Then, the subsection 5.2 presents the estimated parameters, and the voltage and current generated by simulation of the model, and its comparison with real test measurements. Finally, in subsection 5.3 is presented a sensitive analysis of the proposed method, based on the input noise on the test measurements.

5.1. Design of the M-SVR using the training measurements

As explained in Section 3, the electric arc model is represented by the parametric equations (1), (2), (3), and (4). These equations require the estimation of the parameters $\{k_1, k_2, k_3, m, n, s, \delta, \omega, \rho, \kappa, \alpha, R_c, L_c\}$. Now, the following consideration can be applied, in order to reduce the number of parameters to be estimated: the parameters m and n depend on the operating stage of the EAF (boring, melting and refining), therefore, to represent the melting stage of the EAF $m = 0$ and $n = 2$ [39]. This corresponds to the stage where real measurements of the current and the voltage are taken. In the Chua's circuit is a common practice to set the values of ρ, κ and α, to produce a chaotic behavior in the circuit by means of the parameter δ

Table 1: Range of variation of EAF model parameters.

Parameter	Lower Limit	Upper Limit
k_1	3000	7000
k_2	1	5
k_3	4.5	12
s	17	39
δ	14	20
w	0.1	0.5
R_c	1×10^{-4}	10×10^{-4}
L_c	1×10^{-6}	10×10^{-6}

[15], [40]. Therefore in (4), the values of ρ, κ and α are fixed as $-1/7$, $2/7$, and 10, respectively, whereas δ and s are estimated within the ranges [14, 20] and [17, 39], respectively, to produce a low-frequency chaotic signal (within the 0.5 to 25 Hz range) in the circuit solution [15]. After adjusting the values of n, m, ρ, κ and α, the parameters of the electric arc model to be estimated are $\{k_1, k_2, k_3, s, \delta, \omega, R_c, L_c\}$. Considering the description given for the M-SVR in subsection 4.1, the output vector of the M-SVR is $\hat{\mathbf{y}} = [k_1, k_2, k_3, s, \delta, w, R_c, L_c]^\top$.

As mentioned in subsection 4.3, the vectors $\mathbf{y}_i$ are generated using LHS within the space of possible values for each parameter, which is bounded by lower and upper limits. The values of the limits are chosen based on typical data available in [14–16], and [39]. The lower and upper limits for each parameter are listed in Table 1.

To compute the hyperparameters of the M-SVR, are set $N_P = 30$, $F = 0.8$, $CR = 0.5$, and $g^{\max} = 30$ in the DE algorithm. The hyperparameters are searched in the ranges $C = \{1, \ldots, 100\}$, $\epsilon = \{10^{-6}, \ldots, 10^{-3}\}$, and $\sigma = \{1, \ldots, 50\}$. The training dataset $\{(\mathbf{x}_i, \mathbf{y}_i)\}_{i=1}^{N}$ are computed following the proposed method described in subsection 4.3. Different values have been considered for the number of training samples N, in order to determine their effect on the estimated model parameters. For each value of N are estimated the parameters of the electric arc model, related to the training measurements. With these parameters the electric arc model is adjusted, in order to estimate the voltage waveform. The estimated voltage are compared with the training measurements of real voltage through the objective function. In Fig. 6, are shown the values of the OF for different values of the training set size N.

According to the results shown in the Fig. 6, the training samples size used to design the algorithm is related to its performance. If we used a number of samples lower than 60, the values obtained for the objective function are larger than 5, and reduced near to 4.75, when the number of samples is major to 100. We also noted that the best value for the OF is obtained when the training set size is equal to $N = 70$.

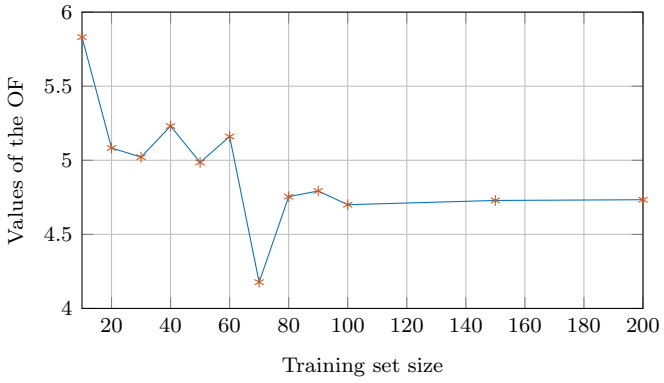

Figure 6: Relation between the OF and the training set size N.

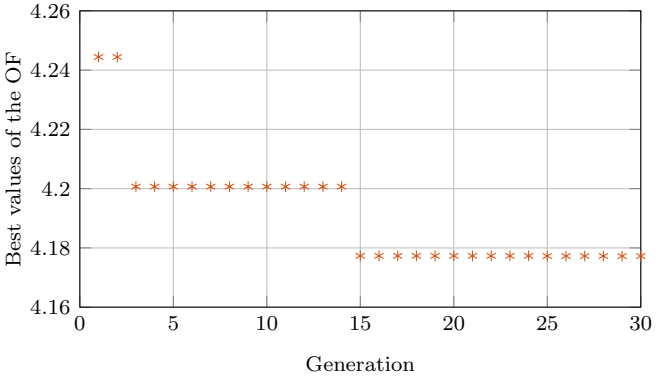

Figure 7: Best value of the OF obtained in each generation, using the DE algorithm.

Based on the above, the proposed method operates satisfactorily with short training size, around 60 to 100 samples.

The results reported in the rest of this paper are obtained with $N = 70$. The values obtained for the hyperparameters are $C = 47.83$, $\epsilon = 10^{-6}$ and $\sigma = 9.35$. Fig. 7 shows the best values of the OF in each generation. It can be seen that, the value of the OF decreases as the number of iteration increases, until it reaches a value 4.18 after the iteration 15. Once the hyperparameters has been calculated, the martrix $\boldsymbol{\beta}$ and the vector $\mathbf{b}$ for the M-SVR are computed with the training data set, as explained in Section 4.1.

5.2. Estimated voltage and current using the testing measurements

In this part, the test measurements are used. For the test measurements of real voltage, its characteristics are computed to obtain the input vector $\mathbf{x}_{\text{real}}$. The estimate parameters of the electric are model ($\hat{\mathbf{y}}$) are obtained by replacing the values of the matrix $\boldsymbol{\beta}$ and the vector $\mathbf{b}$ (computed in the training phase), and $\mathbf{x}_{\text{real}}$ in (2). Table 2 lists the values of the parameters estimated from the output of the M-SVR.

Table 2: Estimated EAF model parameter with test measurements.

	k_1	k_2	k_3	s	δ	w	R_c	L_c
Estimated value	7001.3	5.04	7.8	24.6	21.32	0.13	6.26×10^{-4}	10×10^{-6}

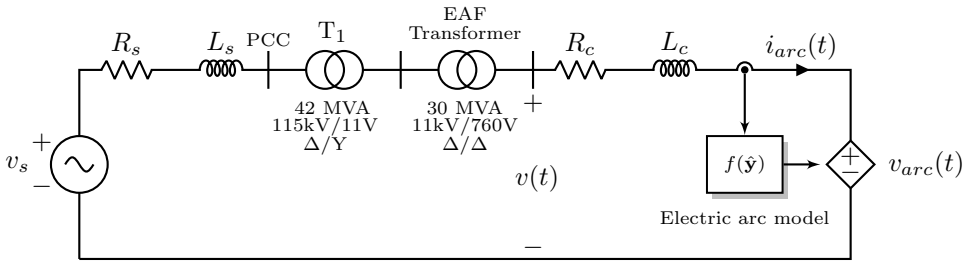

Figure 8: Single-phase diagram of the EAF power system implemented in Matlab/Simulink.

With the estimated parameters, is run a simulation of the EAF circuit shown in Fig. 8, implemented in Matlab/Simulink. The internal voltage v_s is computed as explained in Section 2. The simulated arc current are used as an input of the electric arc model, represented by the function $f(\hat{\mathbf{y}})$, and the phase voltage at the secondary side of the EAF transformer are computed at each step-time of the simulation.

In Fig. 9 ten cycles of the real (solid line) and simulated (dotted line) phase voltage at the secondary side of the EAF transformer are shown. In Fig 10 the real data current waveform (solid line), and the simulated current (dotted line) are shown. In Fig. 11 the RMS values in each cycle of the real (solid line) and simulated (dotted line) voltage waveform are shown. In Fig. 12 the RMS values for real (solid line) and simulated (dotted line) electric arc current are shown.

As it can been seen, the results obtained show that the simulated waveforms of voltage and current are similar to the real waveforms. In particular, the values estimated for the parameters allow the simulation of voltage and current with RMS values very similar to the corresponding real values, for each one of the cycles of the test data.

The mean value of the percentage error in the RMS value of voltage and current has been calculated as,

$$\mathrm{E}_x = \frac{1}{N_c} \sum_{i=1}^{N_c} \frac{|X_{\mathrm{RMS(est)},i} - X_{\mathrm{RMS(real)},i}|}{X_{\mathrm{RMS(real)},i}} \cdot 100\% \tag{19}$$

where $X_{\mathrm{RMS(real)},i}$ is the RMS value of real measured data, $X_{\mathrm{RMS(est)},i}$ is the RMS value of simulated data, corresponding to the i^{th} cycle. X can represent the voltage or current, and N_c is the number of its cycles. The values of E_x obtained for voltage and current are, $E_v = 5.68\%$, and $E_i = 4.5\%$, respectively.

In Fig. 13 are show the $v-i$ characteristic from real (solid line) and simulated (dotted line) measurements data. As it can be seen in Figures (9), (10), and (13), the electric arc model is able to represent the non-

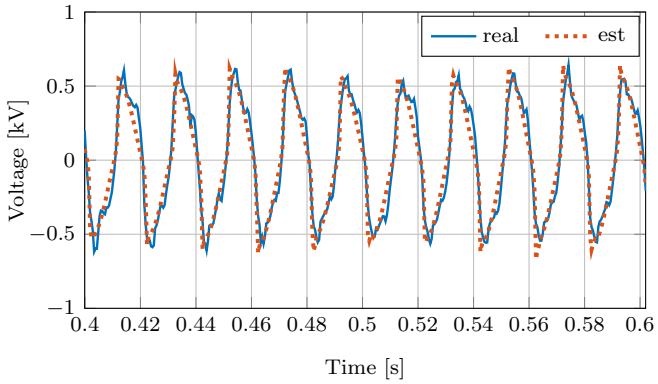

Figure 9: Ten cycles of voltage waveform at the secondary side of the EAF transformer, corresponding to the real data (solid line) and simulated data (dotted line) with the estimated parameters.

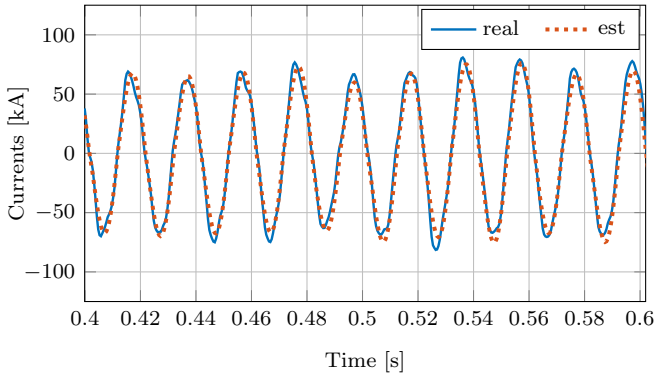

Figure 10: Ten cycles of electric arc current waveform, corresponding to the real data (solid line) and simulated data (dotted line) with the estimated parameters.

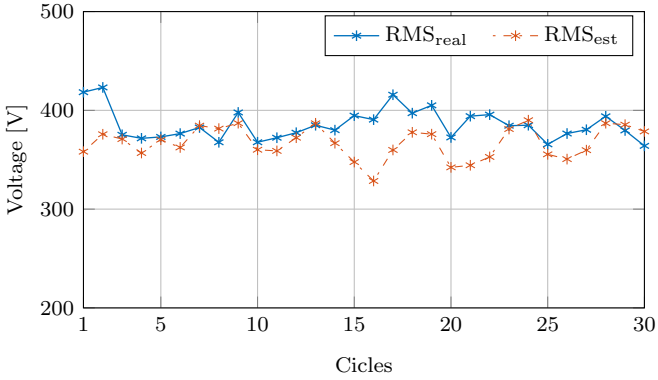

Figure 11: RMS values of voltage at secondary side of EAF transformer in each cycle corresponding to the real data (solid line) and simulated data (dotted line) with the estimated parameters.

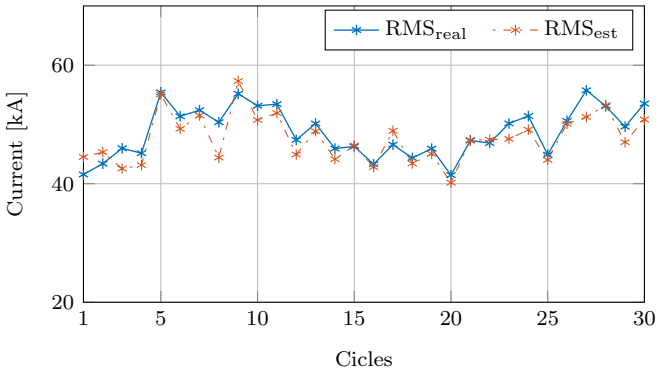

Figure 12: RMS values of electric arc current in each cycle corresponding to the real data (solid line) and simulated data (dotted line) with the estimated parameters.

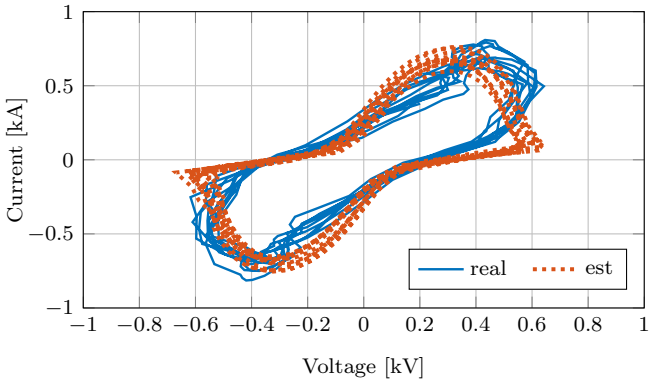

Figure 13: $v - i$ characteristics, corresponding to the real data (solid line), and simulated data (dotted line) with the estimated parameters, during the melting stage of the EAF operation.

linear and time varying nature of the real current and voltage waveform, even during waveform distortion instants.

Fig. 14 shows the components of the characteristic vector, computed as explained in subsection 4.3, for the real (solid line) and simulated (dotted line) voltage. The figure is illustrated over the frequency range [5, 650] Hz. Fig. 15 shows the comparison between the entries from the characteristic vectors of the real (solid line) and simulated (dotted line) current waveform. Notice how the approximation by using the M-SVR is particularly accurate for the largest component, which corresponds to the fundamental frequency of 50 Hz. As shown in Table 3, the relative error between the component at 50 Hz of the characteristic vectors of voltage and current are 6.3%, and 2.1%, respectively, which validates the proper performance of the M-SVR, despite the chaotic dynamic of the EAF operation.

One of the main problems caused by the EAF operation is due to the injection of harmonics and inter-

Table 3: Comparison between the fundamental component of the characteristic vectors of the real and simulated voltage and current.

signal	real	simulated	relative error
current	75.21 kA/Hz	73.58 kA/Hz	2.1%
voltage	58.43 V/Hz	54.69 V/Hz	6.3%

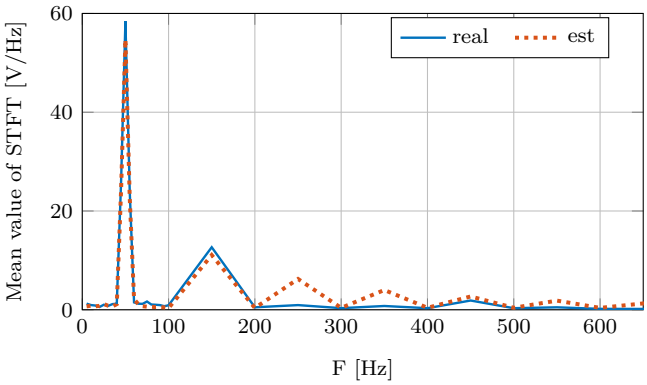

Figure 14: Characteristics of voltage waveform at the secondary side of the EAF transformer, corresponding to the real data (solid line), and simulated data (dotted line) with the estimated parameters.

harmonics in the electrical power system. The total harmonic distortion (THD) index is used to quantify the distortion present in a signal. The THD has been computed using the spectrum of voltages and currents shown in Fig. 14 and Fig. 15, with the following equation

$$\mathrm{THD} = \left(\frac{1}{x_{10}} \sqrt{\sum_{\substack{k=1,\\ k\neq 10}}^{32} x_k^2} \right) \cdot 100\% \tag{20}$$

where x_k $(k = 1, \ldots, 32)$ corresponds to each entry of the characteristic vector, x_{10} corresponds to the main component at the frequency of 50 Hz, and 32 is the number of entries of the characteristic vector. For real voltage measurements the THD is 66.3%, whereas for the simulated voltage is 64.9%. In the case of the current, the THD is 62.2% for real current measurements and 61.9% for the currents obtained with the model. It is worth noting that the high THDs are due to the harmonics and interharmonics that has the spectrum of the signals. As can be seen, the THD is similar between the real and simulated signals, with a relative error of 1.8% for the voltage and 0.4% for the current. This indicates the functionality of the method to estimated the parameters of the model.

Although in this article, the results shown correspond to current and voltage measurements taken in the melting phase of the EAF operation, the proposed method is valid to estimate the arc furnace model

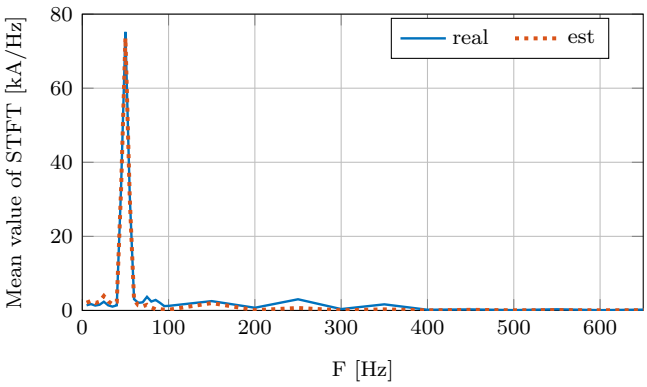

Figure 15: Characteristics of electric arc current waveform, corresponding to the real data (solid line), and simulated data (dotted line) with the estimated parameters.

parameters in the refining stage.

The computation time in each step of the proposed method has been computed using a desktop computer with an Intel(R) Core(TM) processor i5-4210U CPU @ 2.40 GHz. The calculation time is divided into training time and validation time. The training time comprises 68.94 microseconds for the calculation of each vector of parameters using LHS, 4.6 milliseconds for computed each characteristic vector, and 1.25 seconds to evaluated the OF function, given by (18), for each iteration of the DE algorithm. The last task consumes most of the training time (about 6.25 min), due to the large amount of iterations (300 in total). For computing $\boldsymbol{\beta}$ and $\mathbf{b}$, it is necessary 1.2 milliseconds. The computation time in the validation phase is divided into the required time to calculate the characteristics vector from real voltage measurements, which is equal to 2.87 milliseconds, and the required time for the M-SVR to compute the parameters of the EAF model, that is equal to 9.97 microseconds.

5.3. Sensitive analysis based on the input noise on the test measurements

In this section are evaluated the performance of the proposed method for estimating the parameters of the electric arc model, with added Gaussian noise to the test measurements. In Fig. 16 are shown the values of E_x computed usign (19) for voltage (E_v) and current (E_i), considering different values of the signal-to-noise ratios (SNRs) in the test measurements of real voltage and current.

According to the Fig. 16, when measurements with a SNR of less than 5 dB are used, the estimations of the current and voltage present a relative errors larger than 10%, so the proposed method is not appropriate. When the SNR of the measurements is in the range of 5-10 dB, the relative error of the estimated voltage is less than 10%, but the estimated current keeps a relative error major than 10%, this result may be appropriated if less accurate results are sufficient for the analysis. However, the estimation of the voltage and the current is less vulnerable to measurements with a signal to noise ratio larger than 10 dB, they have

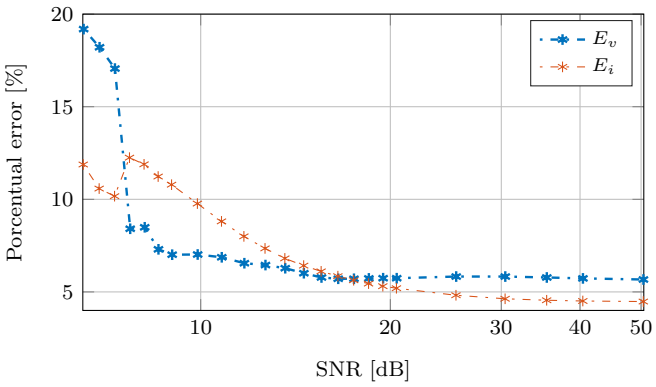

Figure 16: Average values for the relative error of RMS voltage E_v and current E_i in each cycle, for different SNR in the test measurements.

a relative error of less than 10% and decreases asymptotically until it reached the lower limit when the measurements have a signal to noise ratio of 50 dB.

6. Conclusions

In this paper, a new method for parameter estimation of an EAF model has been presented. The model used took into consideration the non-linear and chaotic behavior of the electric arc. According to the obtained results, the proposed method was able to estimate the parameters of an EAF model. The performance of the estimation method was evaluated by comparing the simulated voltage waveform (generated by the EAF model with the estimated parameters), with real voltage measurements from an arc furnace steel plant operating in the melting operating cycle. The results obtained shown high accuracy of the voltage waveform simulated by the EAF model, according to the relative errors of the fundamental component of the voltage (6.3%), and of the electric arc current (2.1%).

Once the methodology has been tested and validated, and the parameters of an EAF model have been tuned appropriately, it would be possible to use the EAF model to predict the voltage of the electric arc. Although in this article, the results shown correspond to current and voltage measurements taken in the melting phase of the EAF operation, the proposed method is valid to estimate the arc furnace model parameters in the refining stage. As future work, the EAF model can be used to assess the performance of different compensation systems such as active power filters, static var compensators, and energy storage systems. Also, it is recommended to evaluate the performance of the M-SVR algorithm, by considering other cost functions such as absolute sum, and weighted absolute sum. Furthermore, the method proposed here could be applied to estimate the parameters of any system of equations that describes the dynamical behavior of an electric arc furnace, for example, the non-linear time-variant resistance model proposed in

[41].

In short, results shown that, with the correct parameters, the proposed EAF modeling is able to capture the dynamics for this type of load, validating the inclusion in a electrical power system for further studies in PQ.

Appendix A. Parameters of electric arc furnace installation shown in Fig. 1

Distribution System: Ideal three-phase sinusoidal ac voltage with phase to phase RMS nominal voltage = 115 kV, X/R ratio: 10. **Transformer T_1:** $\epsilon_{cc} = 12\%$, winding connection: Y/Δ, X/R ratio: 10. **EAF Transformer:** $\epsilon_{cc} = 10\%$, winding connection: Δ/Δ, X/R ratio: 10.

References

[1] M. Gl, O. Salor, B. Alboyaci, B. Mutluer, I. Cadirci, M. Ermis, A new field-data-based EAF model for power quality studies, IEEE Transactions on Industry Applications 46 (3) (2010) 1230–1242. doi:10.1109/TIA.2010.2046280.

[2] L. Hocine, D. Yacine, B. Kamel, K. M. Samira, Improvement of electrical arc furnace operation with an appropriate model, Energy 34 (9) (2009) 1207 – 1214. doi:https://doi.org/10.1016/j.energy.2009.03.003.

[3] A. Sadeghian, J. Lavers, Dynamic reconstruction of nonlinear v-i characteristic in electric arc furnaces using adaptive neuro-fuzzy rule-based networks, Applied Soft Computing 11 (1) (2011) 1448 – 1456. doi:https://doi.org/10.1016/j.asoc.2010.04.016.

[4] E. A. Cano-Plata, A. J. Ustariz-Farfan, O. J. Soto-Marin, Electric arc furnace model in distribution systems, IEEE Transactions on Industry Applications 51 (5) (2015) 4313–4320. doi:10.1109/TIA.2015.2429638.

[5] H. Samet, I. Masoudipour, M. Parniani, New reactive power calculation method for electric arc furnaces, Measurement 81 (Supplement C) (2016) 251 – 263.

[6] D. C. Bhonsle, R. B. Kelkar, Performance evaluation of composite filter for power quality improvement of electric arc furnace distribution network, International Journal of Electrical Power and Energy Systems 79 (2016) 53 – 65. doi:https://doi.org/10.1016/j.ijepes.2016.01.006.

[7] S. M. M. Agah, S. H. Hosseinian, H. A. Abyaneh, N. Moaddabi, Parameter identification of arc furnace based on stochastic nature of arc length using two-step optimization technique, IEEE Transactions on Power Delivery 25 (4) (2010) 2859–2867.

[8] A. T. Teklić, B. Filipović-Grčić, I. Pavić, Modelling of three-phase electric arc furnace for estimation of voltage flicker in power transmission network, Electric Power Systems Research 146 (2017) 218 – 227.

[9] F. Illahi, I. El-Amin, M. U. Mukhtiar, The application of multiobjective optimization technique to the estimation of electric arc furnace parameters, IEEE Transactions on Power Delivery 33 (4) (2018) 1727–1734.

[10] E. Acha, A. Semlyen, N. Rajakovic, A harmonic domain computational package for nonlinear problems and its application to electric arcs, IEEE Transactions on Power Delivery 5 (3) (1990) 1390–1397. doi:10.1109/61.57981.

[11] Yan Wang, Zhizhong Mao, Yan Li, Huixin Tian, Lifeng Feng, Modeling and parameter identification of an electric arc for the arc furnace, in: 2008 IEEE International Conference on Automation and Logistics, 2008, pp. 740–743. doi:10.1109/ICAL.2008.4636247.

[12] D. C. Bhonsle, R. B. Kelkar, Analyzing power quality issues in electric arc furnace by modeling, Energy 115, Part 1 (2016) 830 – 839.

[13] E. O'Neill-Carrillo, G. T. Heydt, E. J. Kostelich, S. S. Venkata, A. Sundaram, Nonlinear deterministic modeling of highly varying loads, IEEE Transactions on Power Delivery 14 (2) (1999) 537–542.

[14] O. Ozgun, A. Abur, Flicker study using a novel arc furnace model, IEEE Trans. Power Del. 17 (4) (2002) 1158–1163.

[15] G. Carpinelli, F. Iacovone, A. Russo, P. Varilone, Chaos-based modeling of dc arc furnaces for power quality issues, IEEE Transactions on Power Delivery 19 (4) (2004) 1869–1876.

[16] A. . Gomez, J. J. M. Durango, A. E. Mejia, Electric arc furnace modeling for power quality analysis, in: 2010 IEEE ANDESCON, 2010, pp. 1–6. doi:10.1109/ANDESCON.2010.5629655.

[17] G. C. Montanari, M. Loggini, A. Cavallini, L. Pitti, D. Zaninelli, Arc-furnace model for the study of flicker compensation in electrical networks, IEEE Transactions on Power Delivery 9 (4) (1994) 2026–2036. doi:10.1109/61.329535.

[18] G. Manchur, C. C. Erven, Development of a model for predicting flicker from electric arc furnaces, IEEE Transactions on Power Delivery 7 (1) (1992) 416–426. doi:10.1109/61.108936.

[19] Y.-J. Liu, G. W. Chang, R.-C. Hong, Curve-fitting-based method for modeling voltage-current characteristic of an ac electric arc furnace, Electric Power Systems Research 80 (5) (2010) 572 – 581. doi:https://doi.org/10.1016/j.epsr.2009.10.015.

[20] J. G. Mayordomo, L. F. Beites, R. Asensi, M. Izzeddine, L. Zabala, J. Amantegui, A new frequency domain arc furnace model for iterative harmonic analysis, IEEE Transactions on Power Delivery 12 (4) (1997) 1771–1778. doi:10.1109/61.634204.

[21] M. T. Esfahani, B. Vahidi, A new stochastic model of electric arc furnace based on hidden Markov model: A study of its effects on the power system, IEEE Transactions on Power Delivery 27 (4) (2012) 1893–1901.

[22] G. W. Chang, C. Chen, Y. Liu, A neural-network-based method of modeling electric arc furnace load for power engineering study, IEEE Transactions on Power Systems 25 (1) (2010) 138–146. doi:10.1109/TPWRS.2009.2036711.

[23] G. W. Chang, M. Shih, Y. Chen, Y. Liang, A hybrid wavelet transform and neural-network-based approach for modelling dynamic voltage-current characteristics of electric arc furnace, IEEE Transactions on Power Delivery 29 (2) (2014) 815–824. doi:10.1109/TPWRD.2013.2280397.

[24] C. Chen, Y. Chen, A neural-network-based data-driven nonlinear model on time-and frequency-domain voltage-current characterization for power-quality study, IEEE Transactions on Power Delivery 30 (3) (2015) 1577–1584. doi:10.1109/TPWRD.2015.2394359.

[25] G. W. Chang, S. Lin, Y. Chen, H. Lu, H. Chen, Y. Chang, An advanced EAF model for voltage fluctuation propagation study, IEEE Transactions on Power Delivery 32 (2) (2017) 980–988.

[26] F. Janabi-Sharifi, G. Jorjani, An adaptive system for modelling and simulation of electrical arc furnaces, Control Engineering Practice 17 (10) (2009) 1202 – 1219. doi:https://doi.org/10.1016/j.conengprac.2009.05.006.

[27] Y. Lee, H. Nordborg, Y. Suh, P. Steimer, Arc stability criteria in ac arc furnace and optimal converter topologies, in: APEC 07 - Twenty-Second Annual IEEE Applied Power Electronics Conference and Exposition, 2007, pp. 1280–1286. doi:10.1109/APEX.2007.357680.

[28] S. Golestani, H. Samet, Generalised cassiemayr electric arc furnace models, IET Generation, Transmission Distribution 10 (13) (2016) 3364–3373. doi:10.1049/iet-gtd.2016.0405.

[29] D. Alkaran, M. Vatani, M. Sanjari, G. Gharehpetian, Parameters estimation of electric arc furnace based on an analytical solution of power balance equation:, International Transactions on Electrical Energy Systems 27 (4) (2016) 1–11. doi:10.1002/etep.2295.

[30] R. Horton, T. A. Haskew, R. F. Burch IV, A time-domain ac electric arc furnace model for flicker planning studies, IEEE Transactions on Power Delivery 24 (3) (2009) 1450–1457. doi:10.1109/TPWRD.2008.2007021.

[31] M. Sánchez-Fernández, M. de Prado-Cumplido, J. Arenas-García, F. Pérez-Cruz, SVM multiregression for nonlinear channel estimation in multiple-input multiple-output systems, IEEE Trans. on Signal Processing 52 (8) (2004) 2298–2307.

[32] M. Kennedy, A. O'Hagan, Bayesian calibration of computer models, Journal of the Royal Statistical Society. Series B (Statistical Methodology) 63 (3) (2001) 425–465.

[33] R. Storn, K. Price, Differential evolution – a simple and efficient heuristic for global optimization over continuous spaces, Journal of Global Optimization 11 (4) (1997) 341–359. doi:10.1023/A:1008202821328.

[34] M. P. Kennedy, Three steps to chaos. i. evolution, IEEE Transactions on Circuits and Systems I: Fundamental Theory and Applications 40 (10) (1993) 640–656.

[35] B. Schölkopf, A. Smola, Learning With Kernels, MIT Press, 2001.

[36] K. Murphy, Machine Learning: A Probabilistic Perspective, Adaptive computation and machine learning series, MIT Press, 2012.

[37] E. Uz-Logoglu, O. Salor, M. Ermis, Online characterization of interharmonics and harmonics of ac electric arc furnaces by multiple synchronous reference frame analysis, IEEE Transactions on Industry Applications 52 (3) (2016) 2673–2683. doi:10.1109/TIA.2016.2524455.

[38] Gustau Camps-Valls, Regression and function approximation, https://www.uv.es/gcamps/software.html, online; accessed 6 June 2020.

[39] M. F. Alves, Z. M. A. Peixoto, C. P. Garcia, D. G. Gomes, An integrated model for the study of flicker compensation in electrical networks, Electric Power Systems Research 80 (10) (2010) 1299 – 1305.

[40] M. P. Kennedy, Three steps to chaos. ii. a chua's circuit primer, IEEE Transactions on Circuits and Systems I: Fundamental Theory and Applications 40 (10) (1993) 657–674.

[41] Tongxin Zheng, E. B. Makram, An adaptive arc furnace model, IEEE Transactions on Power Delivery 15 (3) (2000) 931–939.